sciendo

Civil and Environmental Engineering
Vol. 21, Issue 1, 1-9, DOI: 10.2478/cee-2025-0001

A HIGHER ORDER COMPUTATIONAL MODEL FOR THERMAL ANALYSIS OF ORTHOTROPIC PLATE IN CYLINDRICAL BENDING

Sanjay KULKARNI[1, *]

[1]Civil Engineering Department, Symbiosis Institute of Technology, Symbiosis International (Deemed University), Lavale, Pune-412115, Maharashtra State, India.
[*] corresponding author: sanjay.kulkarni@sitpune.edu.in

Abstract

The one-dimensional analysis of orthotropic plate under cylindrical bending in thermal environment is studied and introduced in this work. In the analysis three cases are considered. In the first case angle between fibre and *x* axis is zero degree. In the second and third cases the angle between fibres and *x* axis are 45^0 and 90^0 respectively. The effect of fibre orientation on thermal stresses and displacements has been studied and presented in this paper. A higher plate theory (HPT) with cubic thickness coordinate as a shape function is used. The equations of motion are derived with the use of virtual work principal. A Navier's technique is used in further solution. The stresses in *x*-*z* plane are evaluated by using equilibrium equations. The FORTRAN-77 software is used to develop a program to evaluate stresses in temperature field. The results obtained are discussed with first order theory (FPT) and classical theory (CPT) for different aspect ratios.

Keywords:

Cylindrical bending
Orthotropic plate
Thermal stresses
Higher order theory
Pure thermal load

1 Introduction

In the domain of structural theories classical thin plate theory omits the transverse shear stress. Whereas these stresses are very effective in laminated plates. In case of first order theory, the shear strains are considered as constant across the thickness of plate. Due to this transverse shear stresses remains constant throughout the thickness. To overcome these effects, higher order theories become essential. The displacement field of present theory represent better cubical equation.

From the literature, sandwich and laminated plates under cylindrical bending is presented by Sayyad and Ghugal [1]. The trigonometric shear deformation theory with the transverse normal effect was used by authors. The mechanical load was considered in the analysis. The peizoelectric laminates with electric potential function under cylindrical bending by using higher order deformation theory is presented by Kant and Shiyekar [2]. This theory includes the normal deformation in the displacement field. The exact solution of laminates under cylindrical bending was given by Pagano [3]. This solution is used as a benchmark for laminates subjected to mechanical load under cylindrical bending. The theory known as discrete layer was hand over by Perel and Palazotto [4] for sandwich plates under cylindrical bending. The theory has the assumption constant transverse strains along thickness direction. Khdeir [5] came out with the solution for vibration of the angle ply laminated plate in cylindrical bending. The author used classical and first order theories for obtaining solution. The 3D elasticity solution for angle ply laminates in cylindrical bending was hand over by Kapuria and Kumari [6]. The bilayer laminated plates under the influence of thermal field are analysed by Ghugal and Kulkarni [7-11]. The auther considered the thermal field as linear and nonlinear through the thicknss. The buckling of laminated plates under mechanical loading by using various shear deformation theories was presented by Fares and Zenkour [12]. The stresses were evaluated in thin orthotropic plate under bending by using generlized differential quadrature method. The method has the effect of thermal strain and transverse load presented by Jane and Hong [13]. Garg et. al [14] presented a new scaled boundary finite element method for thick laminated plates in cylindrical bending. The authers used a plain strain condition approach to prepare a model. Sayyad and Ghugal [15] worked on the performance of the nth

© Author(s) 2024. This work is distributed under the Creative Commons BY 4.0 license (https://creativecommons.org/licenses/by/4.0/).

order shear deformation theory when applied to laminated plates in cylindrical bending. Bhaskar et. al [16] hand over the 3D exact solution for three layer laminated plates in cylindrical bending under thermal load. A higher order stiff shell element has been developed by Sheth and Joshi [17] for the analysis of stiff laminated plates. The static analysis of stiff laminated plate is presented by using new shell element. A study of stress concentration in rectangular laminated plates with different shaped holes within the laminated plates by using finite element method was presented by Yasin et. al [18]. The analysis was presented for angle ply and four layer rectangular plates.

However, orthotropic plate under cylindrical bending in thermal environment and by using higher order plate theory is mearge in literature. Hence, in this paper the study of of orthotropic plate in cylindrical bending under thermal enviromnent and the performance of higher order plate theory (HPT) is presented.

2 Theoretical Formulation

Consider an orthotropic plate in cylindrical bending as shown in figure 1. The dimension of plate along y direction is represented by (b) and the dimension of the plate along x direction is represented by (a). The dimension of plate along y direction is very long as compared to the dimension along x direction. Hence, the plate is in cylindrical bending and the derivatives along y direction becomes zero and ultimately the displacement along y direction equals to zero. In the figure 1, u and w are the axial and transverse displacements along x and z directions respectively. The z direction is considered as positive in downward direction. The top of the plate is subjected to thermal load T (x, z). In the present case a single layer orthotropic plate under cylindrical bending is considered for the thermo-elastic flexural analysis.

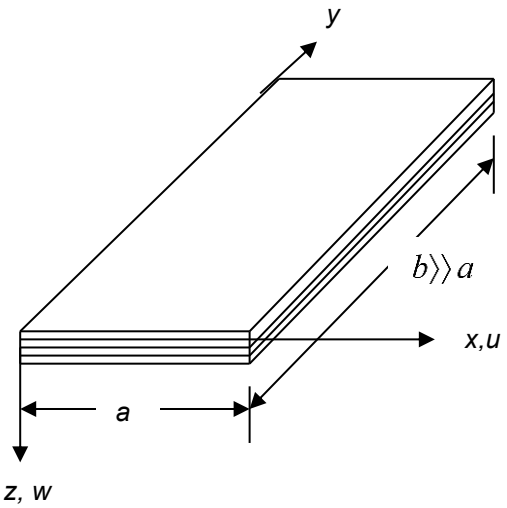

Fig. 1: Cylindrical bending of orthotropic plate and coordinate system

The inplane and transverse displacement of present theory is of the form [12] and can be expressed as follows. The displacement field represented by equations (1) and (2) represents a better kinematic in cubic equation.

$$u(x,z) = z\psi + z^3 \frac{\partial w}{\partial x} + z^3\psi \tag{1}$$

$$w(x) = w(x) \tag{2}$$

In the above displacement field (u, w) represents axial displacement along *x* and transverse displacement along *z*. The term (ψ) is the slope because of bending in the *xz* plane. The strain displacements are given as below has a reference of elasticity theory. These strains are represented by equations (3) and (4).

$$\varepsilon_x = \frac{\partial u}{\partial x} = z\frac{\partial \psi}{\partial x} + z^3 \frac{\partial^2 w}{\partial x^2} + z^3 \frac{\partial \psi}{\partial x} \tag{3}$$

$$\gamma_{zx} = \frac{\partial u}{\partial z} + \frac{\partial w}{\partial x} = \psi + 3z^2\psi + (3z^2 + 1)\frac{\partial w}{\partial x} \tag{4}$$

The thermal effect is introduced and the effect is shown in the strain as below. The normal stress $(\bar{\sigma}_x)$ and transverse shear stress (τ_{zx}) is written in the following matrix form.

$$\begin{Bmatrix} \sigma_x \\ \tau_{zx} \end{Bmatrix} = \begin{bmatrix} \overline{Q}_{11} & 0 \\ 0 & \overline{Q}_{55} \end{bmatrix} \begin{Bmatrix} \varepsilon_x - \alpha_x T \\ \gamma_{zx} \end{Bmatrix} \tag{5}$$

In the above equation (5) the stiffness coefficients $\overline{Q}_{ij}$ are as given below.

$$\overline{Q}_{11} = Q_{11}\cos^4\theta + 2(Q_{12} + 2Q_{66})\sin^2\theta\cos^2\theta + Q_{22}\sin^4\theta \tag{6}$$

$$\overline{Q}_{55} = Q_{55}\cos^2\theta + Q_{44}\sin^2\theta \tag{7}$$

The equation (6) and (7) are in terms of cosine angles. These equations are used to compute the stiffness coefficients when angle between fiber axis or material axis is in between zero and 90 degrees.

$$Q_{11} = \frac{E_1}{1-\mu_{12}\mu_{21}},\ Q_{12} = \frac{\mu_{12}E_2}{1-\mu_{12}\mu_{21}},\ Q_{22} = \frac{E_2}{1-\mu_{12}\mu_{21}} \tag{8}$$

$$Q_{66} = G_{12},\quad Q_{44} = G_{23},\quad Q_{55} = G_{13} \tag{9}$$

The above equations (8) and (9) are used when fibers are parallel to reference axis *x*. This means the angle between fiber and *x* axis is zero.

The transformed thermal coefficient α_x is given by following equation (10).

$$\alpha_x = \alpha_1\cos^2\theta + \alpha_2\sin^2\theta \tag{10}$$

The angle between material axis 1 and reference axis *x* is represented by θ and shown in fig 2.

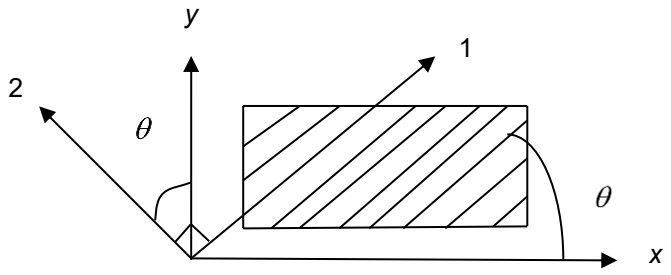

Fig. 2: A fiber reinforced lamina

In the above figure 2, The axis 1 is along fiber and axis 2 is normal to axis 1. These two axes are mutually perpendicular to each other and are known as material axes. The reference axes are represented by *x, y*. In the present study the angle between material axis 1 (fiber) and reference axis *x* is considered as zero, 45 degree and 90 degree during thermal bending analysis of orthotropic plate under cylindrical bending.

The temperature field given by following equation is taken into consideration during the thermal analysis.

$$T(x,z) = 2\frac{z}{h}T_0\sin\frac{\pi x}{a} \tag{11}$$

The above equation (11) represents a linear variation of temperature across the thickness of plate under cylindrical bending. The above temperature field is a function of x and z.

3 Equations of Motion

The virtual work principal along finite dimension and across the thickness of plate strip has been applied and obtained as below:

$$\int_{-\frac{h}{2}}^{\frac{h}{2}} \int_{0}^{a} \left(\sigma_x \delta\varepsilon_x + \tau_{zx}\delta\gamma_{zx}\right)\, dx dz = 0 \tag{12}$$

The symbol δ in the above equation (12) is variational operator and collecting the coefficients of $\delta w, \delta\psi$ the equations of motion are obtained as follows.

$$\delta w : D_1 \frac{\partial^3 \psi}{\partial x^3} + D_2\left(\frac{\partial^4 w}{\partial x^4} + \frac{\partial^3 \psi}{\partial x^3}\right) - D_3 \frac{\partial \psi}{\partial x} - D_4 \frac{\partial \psi}{\partial x} - D_5 \frac{\partial^2 w}{\partial x^2} = D_{10} \frac{\partial^2 T_0}{\partial x^2} \tag{13}$$

$$\delta\psi : -D_1\left(\frac{\partial^3 w}{\partial x^3} + \frac{\partial^2 \psi}{\partial x^2} + \frac{\partial^2 \psi}{\partial x^2}\right) - D_2\left(\frac{\partial^3 w}{\partial x^3} + \frac{\partial^2 \psi}{\partial x^2}\right) + D_3 \frac{\partial w}{\partial x} + D_4 \frac{\partial w}{\partial x} - D_6 \frac{\partial^2 \psi}{\partial x^2} + D_7 \psi + \psi\left(2D_8 + D_9\right) = -D_{11} \frac{\partial T_0}{\partial x} \tag{14}$$

The coefficients appeared in the above equations of motion (13) - (14) of an orthotropic plate strip are given below.

$$D_1 = Q_{11}\frac{h^5}{80},\ D_2 = Q_{11}\frac{h^7}{448},\ D_3 = Q_{55}\left(\frac{3h^3}{12} + h\right),\ D_4 = Q_{55}\left(\frac{9h^5}{80} + \frac{3h^3}{12}\right),$$

$$D_5 = Q_{55}\left(\frac{9h^5}{80} + h + \frac{6h^3}{12}\right),\ D_6 = Q_{11}\frac{h^3}{12},\ D_7 = hQ_{55},\ D_8 = 3Q_{55}\frac{h^3}{12},\ D_9 = Q_{55}\frac{9h^5}{80},$$

$$D_{10} = Q_{11}\alpha_x \frac{2h^5}{80h},\ D_{11} = Q_{11}\alpha_x \frac{2}{h}\left(\frac{h^3}{12} - \frac{h^5}{80}\right)$$

The performance of the theory is studied by analyzing a plate strip under single sinusoidal thermal load. The material properties are considered as below.

$$\frac{E_1}{E_2} = 25,\ G_{12} = G_{13} = 0.5E_2,\ \mu_{12} = 0.25,\ \frac{\alpha_2}{\alpha_1} = 3$$

Where, α_1 and α_2 are coefficients of thermal expansion along material axes i.e. in the fiber direction and transverse direction respectively as shown in figure 2. The modulus of elasticity along material axes 1 and 2 is represented by E_1 and E_2 respectively. The shear modulus and Poisson's effect are denoted by G_{ij} and μ_{ij} respectively.

4 The solution scheme

The closed-formed Navier's technique is used for orthotropic plate in cylindrical bending. The solution satisfying the boundary conditions is given below.

$$w(x) = \sum_{m=1}^{\infty} w_m \sin\frac{m\pi x}{a} \tag{15}$$

$$\psi(x) = \sum_{m=1}^{\infty} \psi_m \cos\frac{m\pi x}{a} \tag{16}$$

The arbitrary constants in the above solution is shown by w_m, ψ_m. The expansion of thermal load is in Fourier single sine series as given below.

$$T_0(x) = \sum_{m=1}^{\infty} T_{0m} \sin\frac{m\pi x}{a} \tag{17}$$

For sinusoidal temperature field $(m=1)$, and the coefficient leads to $T_{0m} = T_0$, where the maximum thermal field intensity is T_o. Put the solution obtained from equations (15)-(17) into equations of motion (13)-(14) results into a set of algebraic equations. These equations one can write into a matrix form as follows:

$$[K]\{\delta\} = \{f\} \tag{18}$$

The matrix $[K]$ in the equation (18) is known as stiffness matrix (symmetric), $\{\delta\}=\{w_m,\psi_m\}$ and $\{f\}$ is known as force matrix. The unknown coefficients $\{\delta\}$ can be evaluated by solving the above set of equations. The thermal displacements and stresses can be obtained by putting coefficients into equations (15).

The stiffness matrix $[K]$ and corresponding coefficients are as given below.

$$[K]=\begin{bmatrix} K_{11} & K_{12} \\ K_{21} & K_{22} \end{bmatrix} \tag{19}$$

$$K_{11}=D_2\frac{m^4\pi^4}{a^4}+D_5\frac{m^2\pi^2}{a^2} \tag{20}$$

$$K_{12}=D_1\frac{m^3\pi^3}{a^3}+D_2\frac{m^3\pi^3}{a^3}+D_3\frac{m\pi}{a}+D_4\frac{m\pi}{a} \tag{21}$$

$$K_{21}=D_1\frac{m^3\pi^3}{a^3}+D_2\frac{m^3\pi^3}{a^3}+D_3\frac{m\pi}{a}+D_4\frac{m\pi}{a} \tag{22}$$

$$K_{22}=D_6\frac{m^2\pi^2}{a^2}+2D_1\frac{m^2\pi^2}{a^2}+D_2\frac{m^2\pi^2}{a^2}+D_7+2D_8+D_9 \tag{23}$$

The elements of stiffness matrix $[K]$ are shown in equations from (19) to (23).

The force matrix $\{f\}$ is represented by equations (24) as given below.

$$\{f\}=\begin{Bmatrix} f_1 \\ f_2 \end{Bmatrix} \tag{24}$$

$$f_1=-D_{10}\frac{m^2\pi^2}{a^2}T_{0m} \tag{25}$$

$$f_2=-D_{11}\frac{m\pi}{a}T_{0m} \tag{26}$$

The equations (25) and (26) represents the elements of force matrix.

5 Numerical Results and discussions

The numerical results are computed by using higher order (HPT), first order (FPT) and classical plate (CPT) theories for an orthotropic plate in cylindrical bending under thermal environment for aspect ratios 4 and 10. The locations of axial displacement ($\bar{u}$), transverse displacement ($\bar{w}$), normal stress ($\bar{\sigma}_x$) and transverse shear stress ($\bar{\tau}_{zx}^{CR}$) are shown in following dimensionless form. These results are tabulated in table 1 and table 2.

$$\bar{u}\left(0,-\frac{h}{2}\right)=\frac{u}{\alpha_1 T_0 a},\quad \bar{w}\left(\frac{a}{2},0\right)=\frac{10\times h\times w}{\alpha_1 T_0 a^2},\quad \bar{\sigma}_x\left(\frac{a}{2},-\frac{h}{2}\right)=\frac{\sigma_x}{E_2\alpha_1 T_0},\quad \bar{\tau}_{zx}(0,0)=\frac{\tau_{zx}}{E_2\alpha_1 T_0}$$

Table 1: Non-dimensional displacements and stresses for an orthotropic plate in cylindrical bending under linear thermal load for aspect ratio 4.

θ	Throry	Aspect Ratio	$\bar{u}$	$\bar{w}$	$\bar{\sigma}_x$	$\bar{\tau}_{zx}^{CR}$
0^0	HPT	4	0.3123	1.9875	0.1247	-0.0006
	FPT		0.3183	2.0264	0.0000	0.0000
	CPT		0.3183	2.0264	0.0000	-
45^0	HPT	4	0.6247	3.9761	0.0710	-0.0003
	FPT		0.6366	4.0528	0.0000	0.0000
	CPT		0.6366	4.0528	0.0000	-
90^0	HPT	4	0.9370	5.9650	0.0150	-0.0001
	FPT		0.9549	6.0793	0.0000	0.0000
	CPT		0.9549	6.0793	0.0000	-

Table 2: Non-dimensional displacements and stresses for an orthotropic plate in cylindrical bending under linear thermal load for aspect ratio 10.

θ	Throry	Aspect Ratio	$\overline{u}$	$\overline{w}$	$\overline{\sigma}_x$	$\overline{\tau}_{zx}^{CR}$
0^0	HPT	10	0.3174	2.0203	0.0191	0.0000
	FPT		0.3183	2.0264	0.0000	0.0000
	CPT		0.3183	2.0264	0.0000	-
45^0	HPT	10	0.6347	4.0407	0.0109	0.0000
	FPT		0.6366	4.0528	0.0000	0.0000
	CPT		0.6366	4.0528	0.0000	-
90^0	HPT	10	0.9521	6.0610	0.0023	0.0000
	FPT		0.9549	6.0793	0.0000	0.0000
	CPT		0.9549	6.0793	0.0000	-

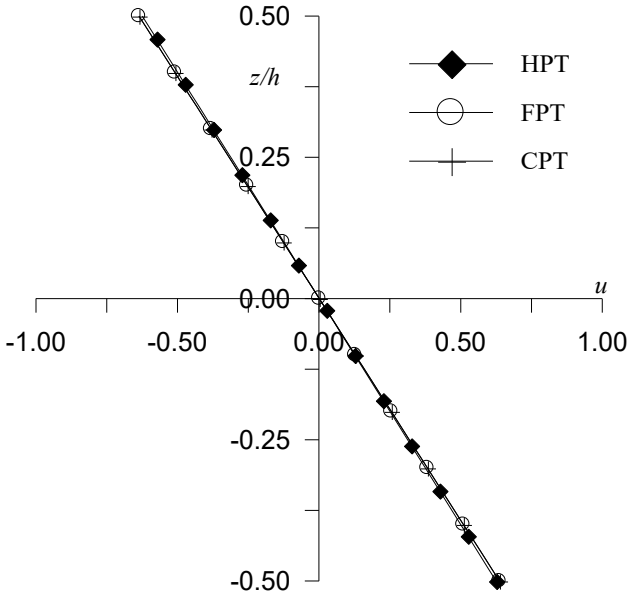

Fig. 3: Normalized axial displacement ($\overline{u}$) in plate under cylindrical bending when fibres are oriented at $+45^0$ to *x* axis for aspect ratio 4

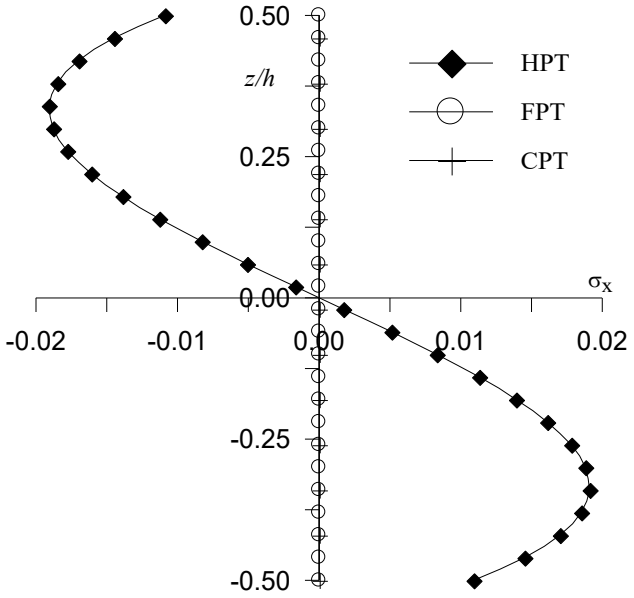

Fig. 4: Dimensionless normal stress ($\overline{\sigma}_x$) in plate under cylindrical bending when fibres are oriented at $+45^0$ to *x* axis for aspect ratio 10.

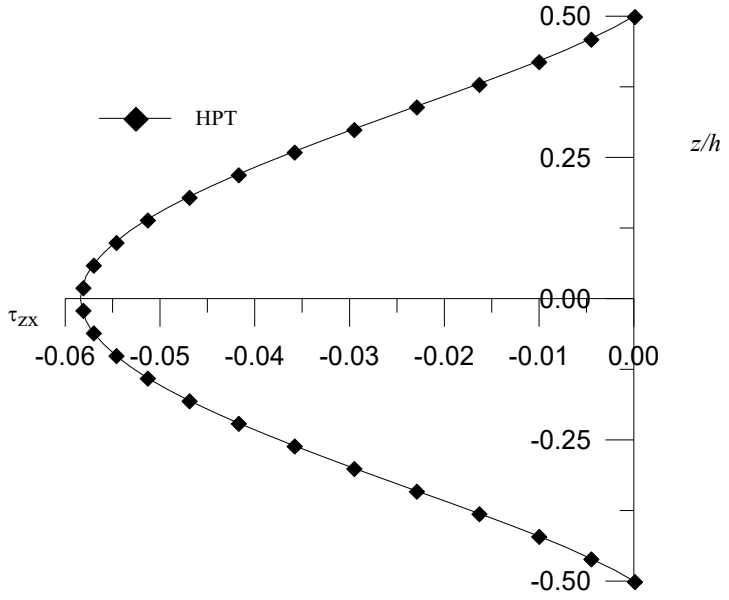

Fig. 5: Dimensionless transverse shear stress ($\overline{\tau}_{zx}^{EE}$) evaluated by equilibrium equations in plate in cylindrical bending when fibres are oriented at 0^0 to *x* axis for aspect ratio 4.

Axial Displacement $(\overline{u})$: The results of axial displacement along *x* axis obtained by higher order plate theory (HPT) are in line with first order and classical theory for aspect ratios 4 and 10. It is seen that axial displacement increases slightly when aspect ratio changes from 4 to 10, whereas the axial displacements obtained by first order plate theory (FPT) and classical plate theory (CPT) does not display any change in the results even after the aspect ratio changes from 4 to 10. The axial displacement increases as the fiber orientation increases with *x* axis. The through thickness variation of inplane displacement is shown in figure 3 under pure thermal load.

Transverse Displacement $\left(\overline{w}\right)$: Transverse displacement under linear thermal load obtained by higher order plate theory (HPT) shows the lower value as compared to the result obtained by first order plate theory (FPT) and classical plate theory (CPT). This indicates that HPT under predicts the transverse displacements, whereas FPT and CPT slightly over predicts the transverse displacements for aspect ratios 4 and 10. Transverse displacements obtained by first order plate theory and classical plate theory are irrespective of their aspect ratios.

Axial Normal Stress $\left(\overline{\sigma}_x\right)$: The pure thermal load effect on axial normal stress is not seen as the results of axial normal stress obtained by FPT and CPT in thermal environment are zero for aspect ratios 4 and 10, whereas the normal stresses are not zeros when obtained by higher order theory (HPT). The variation of normal stresses across the thickness is shown in fig.4. The curve is seen in the figure 4.

Transverse Shear Stresses $\left(\overline{\tau}_{zx}^{CR}\right)$: The constitutive relationship (CR) and equations of equilibrium are used to find transverse shear stresses. Transverse shear stresses are observed as zero by first order plate theory; whereas transverse shear stresses obtained by HPT are less than zero when evaluated from constitutive relationship. The stress-free boundary conditions are fulfilled when transverse shear stresses ($\overline{\tau}_{zx}^{EE}$) are estimated by using equations of equilibrium. The through thickness variation of these stresses are shown in figure 5. The realistic curve is obtained fulfilling the condition of zero stress at the top and bottom of the plate in cylindrical bending.

6 Conclusion

The flexural response of orthotropic plate in cylindrical bending under thermal environment is investigated by using higher order plate theory. It has been observed that there is a significant rise in thermal displacements under linear thermal load, whereas the thermal stresses do not show any significant change in results under linear thermal load. The normal stresses obtained by HPT shows realistic curve through the thickness where as FPT and CPT shows zero normal stresses across the thickness. This indicates that the effect of linear thermal load on normal stresses obtained by FPT and CPT is negligible. First order and classical theory slightly over predicts thermal displacements and under predicts stresses under linear thermal load.

Acknowledgement

We are thankful to Symbiosis Institute of Technology, Pune for continuous support and encouragement to complete this work.

References

[1] SAYYAD, A.S. – GHUGAL, Y.M.: Cylindrical bending of multilayered composite laminates and sandwiches. Advances in Aircraft and Spacecraft Science, Vol. 3, Iss. 2, 2016, pp. 113-148, http://dx.doi.org/10.12989/aas.2016.3.2.113

[2] KANT, T. - SHIYEKAR, S.M.: Cylindrical bending of piezoelectric laminates with a higher order shear and normal deformation theory. Computers and Structures, Vol. 86, 2008, pp. 1594-1603, https://doi.org/10.1016/j.compstruc.2008.01.002.

[3] PAGANO, N.J.: Exact solution for composite laminates in cylindrical bending. Journal of Composite Materials, Vol. 3, 1969, pp. 398-411.

[4] PERELI, V.Y. - Palazotto, A.N.: Finite element formulation for cylindrical bending of a transversely compressible sandwich plate based on assumed transverse strain. International Journal of Solids and Structures, Vol. 38, 2001, pp. 5373-5409, https://doi.org/10.1016/S0020-7683(00)00293-6.

[5] KHDEIR, A.A.: Free and forced vibration of antisymmetric angle ply laminated plate strips in cylindrical bending. Journal of Vibration and Control, Vol. 7, 2001, pp. 781-801, http://dx.doi.org/10.1177/107754630100700602

[6] KAPURIA, S. - Kumari, P.: Extended Kantorovich method for three-dimensional elasticity solution of laminated composite structures in cylindrical bending. Journal of Applied Mechanics, Vol. 78, Iss. 6, 2011, pp. 1-8, https://doi.org/10.1115/1.4003779.

[7] GHUGAL, Y.M. - KULKARNI, S.K.: Thermal response of symmetric cross-ply laminated plates subjected to linear and nonlinear thermo-mechanical loads. Journal of Thermal Stresses, Vol. 36, Iss. 5, 2013, pp. 466-479, https://doi.org/10.1080/01495739.2013.770664.

[8] GHUGAL, Y.M. - KULKARNI, S.K.: Flexural analysis of cross ply laminated plates subjected to nonlinear thermal and mechanical loadings. Acta Mechanica, Vol. 224, Iss. 3, 2013, pp. 675-690, https://doi.org/10.1007/s00707-012-0774-1.
[9] GHUGAL, Y.M. - KULKARNI, S.K.: Thermal flexural analysis of cross ply laminated plates using trigonometric shear deformation theory. Latin American Journal of Solids and Structures, Vol. 10, 2013, pp. 1001–1023, https://doi.org/10.1590/S1679-78252013000500008.
[10] GHUGAL, Y.M. - Kulkarni, S.K.: Thermal stress analysis of cross ply laminated plates using refined shear deformation theory. Journal of Experimental and Applied Mechanics, Vol. 2, Iss. 1, 2011, pp. 47-66.
[11] KULKARNI, S.K. - GHUGAL, Y.M.: Effect of degree of orthotropy on transverse deflection of composite laminates under thermal load. Advances in Structural Engineering, doi: 10.1007/978-81-322-2190-6_15 (2015) 157-169.
[12] FARES, M.E. - ZENKOUR, A.M.: Buckling and free vibration of non-homogeneous composite cross ply laminated plates with various plate theories. Composite Structures, Vol. 44, 1999, pp. 279-287, 10.1016/s0263-8223(98)00135-4.
[13] JANE, K.C. - HONG, C.C.: Thermal bending analysis of laminated orthotropic plates by the generalized differential quadrature method. Mechanics Research Communications, Vol. 27, Iss. 2, 2000, pp. 157-164, https://doi.org/10.1016/S0093-6413(00)00076-8.
[14] GARG, N. - PRUSTY, B. G. – SONG, C. - PHILLIPS, A.W.: Cylindrical bending of thick laminated composite plates using scaled boundary finite element method. Engineering Analysis with Boundary Elements, Vol. 120, 2020, pp. 73-81, https://doi.org/10.1016/j.enganabound.2020.08.009.
[15] SAYYAD, A. S. - GHUGAL, Y. M.: A nth order shear deformation theory for composite laminates in cylindrical bending. Curved and Layered Structures. Vol. 2, Iss. 1, 2015, pp. 290-300, http://dx.doi.org/10.1515/cls-2015-0016.
[16] BHASKAR, K. - Varadan, T. K. - Ali, J. S. M.: Thermoelastic solutions for orthotropic and anisotropic composite laminates. Composite: Part B 27B. 1996, pp. 415-420, https://doi.org/10.1016/1359-8368(96)00005-4.
[17] SHETH, K. - JOSHI, R.: Development of higher order stiffened shell element (HOST9) for the static analysis of stiffened laminated plates. Civil and Environmental Engineering. Vol. 20, Iss. 1, 2024, pp. 217-232, https://doi.org/10.2478/cee-2024-0018.
[18] YASIN, B. - QI'DAN, D. - Al-OLIMAT, S. - AVASRAH, M. - ALMASAEID, H.: Effect of the fibre orientation angles on stress concentration around various shapes of hole in laminated composite plate subject to in-plane loading. Civil and Environmental Engineering. Vol. 19, Iss. 1, 2023, pp. 218-223, https://doi.org/10.2478/cee-2023-0019.